NASA TECHNICAL NOTE
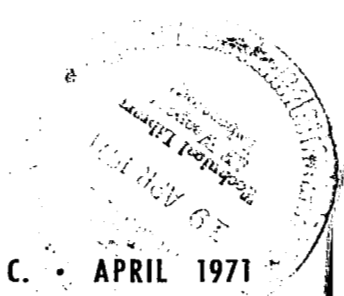
NASA TN D-6195

A WIND-TUNNEL INVESTIGATION OF SONIC-BOOM PRESSURE DISTRIBUTIONS OF BODIES OF REVOLUTION AT MACH 2.96, 3.83, AND 4.63

by Barrett L. Shrout, Robert J. Mack, and Samuel M. Dollyhigh

Langley Research Center
Hampton, Va. 23365

1. Report No. NASA TN D-6195	2. Government Accession No.	3. Recipient's Catalog No.
4. Title and Subtitle A WIND-TUNNEL INVESTIGATION OF SONIC-BOOM PRESSURE DISTRIBUTIONS OF BODIES OF REVOLUTION AT MACH 2.96, 3.83, AND 4.63		5. Report Date April 1971
		6. Performing Organization Code
7. Author(s) Barrett L. Shrout, Robert J. Mack, and Samuel M. Dollyhigh		8. Performing Organization Report No. L-7398
9. Performing Organization Name and Address NASA Langley Research Center Hampton, Va. 23365		10. Work Unit No. 126-13-11-03
		11. Contract or Grant No.
12. Sponsoring Agency Name and Address National Aeronautics and Space Administration Washington, D.C. 20546		13. Type of Report and Period Covered Technical Note
		14. Sponsoring Agency Code

15. Supplementary Notes

16. Abstract

Sonic-boom pressure signature measurements were made for a series of bodies of revolution at Mach numbers of 2.96, 3.83, and 4.63. Maximum overpressure and signature impulse tend to increase with increasing Mach number as predicted by a near-field modified linear theory applicable to smooth bodies. However, the measured signatures agree only qualitatively with near-field theory at the high Mach numbers. Inclusion in the theory of the effects of oblique-plane-surface forces and model boundary layer improved the correlation between theory and experiment. A nonsmooth-body theory produced better agreement for the trailing shock but with some reduction of the signature impulse.

17. Key Words (Suggested by Author(s)) Sonic boom Bodies of revolution Near-field theory	18. Distribution Statement Unclassified – Unlimited		
19. Security Classif. (of this report) Unclassified	20. Security Classif. (of this page) Unclassified	21. No. of Pages 32	22. Price* $3.00

*For sale by the National Technical Information Service, Springfield, Virginia 22151

A WIND-TUNNEL INVESTIGATION OF
SONIC-BOOM PRESSURE DISTRIBUTIONS OF BODIES
OF REVOLUTION AT MACH 2.96, 3.83, AND 4.63

By Barrett L. Shrout, Robert J. Mack,
and Samuel M. Dollyhigh
Langley Research Center

SUMMARY

Sonic-boom pressure signature measurements were made for a series of bodies of revolution at Mach numbers of 2.96, 3.83, and 4.63. Maximum overpressure and signature impulse tend to increase with increasing Mach number as predicted by a near-field modified linear theory applicable to smooth bodies. However, the measured signatures agree only qualitatively with near-field theory at the high Mach numbers. Inclusion in the theory of the effects of oblique-plane-surface forces and model boundary layer improved the correlation between theory and experiment. A nonsmooth-body theory produced better agreement for the trailing shock but with some reduction of the signature impulse.

INTRODUCTION

Research on sonic-boom phenomena until recently has been concentrated in the supersonic Mach number range from 1.0 to 3.0 where current military aircraft are flying and where the supersonic transport will fly. Theoretical methods for estimating the sonic boom within this speed range have been developed and verified, and techniques for reducing the sonic boom have been analyzed.

Current interest in the hypersonic transport has created a need for information about the sonic boom at higher Mach numbers, where linear theory may no longer apply. Information to be obtained includes maximum overpressures, signature impulse, and the near-field or far-field characteristics of the pressure signatures. In addition, test procedures can be established and the adequacy of existing theories in estimating the pressure signature characteristics can be evaluated.

An earlier investigation of the effects of body shape on sonic-boom pressure distributions for the Mach number range 1.25 to 2.0 is reported in reference 1. Three of the body shapes from that series of tests were chosen for the present investigation, including a cone, a body having a linear distribution of area, and a body having an area distribution

which (based on the theory of ref. 2) produces the lower bound of maximum overpressure for far-field conditions. For each body shape, three models were constructed with progressively increasing base area that represented in nondimensionalized form the maximum equivalent areas of a supersonic transport during transonic acceleration, a supersonic transport during cruise, and a hypersonic transport during cruise.

The nine models were tested in the Langley Unitary Plan wind tunnel at Mach numbers of 2.96, 3.83, and 4.63. The results of these tests and the corresponding theoretical analysis are presented herein.

SYMBOLS

Values are given in both SI and U.S. Customary Units. The measurements and calculations were made in U.S. Customary Units.

A cross-sectional area of model determined by supersonic-area-rule cutting planes having an angle μ with respect to longitudinal axis

A_{ref} reference area, base area of smallest models, 0.258 cm^2 (0.04 sq in.)

$A(t)$ nondimensionalized cross-sectional area A/l^2 at nondimensionalized station $t = x/l$

B equivalent cross-sectional area due to lift, $\dfrac{\beta}{2q} \displaystyle\int_0^x \Delta L \, dx$

$B(t)$ nondimensionalized equivalent cross-sectional area due to lift B/l^2 at nondimensionalized station $t = x/l$

C_p surface pressure coefficient, $\dfrac{p_s - p}{q}$

$F(\tau)$ Whitham's F function, $\dfrac{1}{2\pi} \displaystyle\int_0^\tau \dfrac{A''(t)}{\sqrt{\tau - t}} \, dt$

h perpendicular distance from model in negative Z-direction to measuring probe

k constant in body-shape equation

l model reference length, 5.08 cm (2 in.)

L distribution of oblique force term equivalent to lift distribution

2

M   Mach number

n   bluntness parameter (exponent of x in body-shape equation)

p   free-stream static reference pressure

p_s surface pressure

Δp incremental pressure due to flow field of model

Δp_{max} maximum value of Δp

q   free-stream dynamic pressure

r   radius of model

t   dummy variable of integration measured in same direction and using same
           units as τ

X, Y, Z   Cartesian coordinate axes with origin at model nose, X positive downstream
           (see fig. 2)

x   distance along longitudinal axis from model nose

ΔX distance from point on pressure signature to point where pressure-signature
           curve crosses zero-pressure reference axis

$\beta = \sqrt{M^2 - 1}$

μ Mach angle, $\sin^{-1} \dfrac{1}{M}$

τ nondimensionalized distance measured along longitudinal axis from model
           nose, x/l

Δ denotes increment

Subscript:

max   maximum

3

A prime is used to indicate a first derivative and a double prime is used to indicate a second derivative with respect to distance along the model axis.

MODELS, APPARATUS, AND TESTS

The nine models tested in this investigation are illustrated in figure 1 with the equations defining their forebodies. Each model consists of a forebody which is 5.08 cm (2 in.) long and a circular cylinder afterbody approximately 20.32 cm (8 in.) long. The diameter of the cylindrical portion of the model is the same as the maximum diameter of the forebody.

Three forebody shapes were included in the investigation, including a cone, a forebody with a linear increase in area, and a forebody having a distribution of area which, based on the theory of reference 2, gives a lower bound far-field sonic-boom overpressure. For the remainder of this paper these forebody shapes will be referred to as conical, linear, and blunt, respectively. Models of each forebody shape were constructed having base area ratios $\left(A_{max}/A_{ref}\right)$ of 1, 2, and 4 where A_{ref} is 0.258 cm^2 (0.04 in^2). It should be noted that models 1, 2, and 3 of this investigation are identical to models 1, 4, and 5, respectively, of reference 1.

A sketch of the wind-tunnel test apparatus is shown in figure 2. The model actuator, mounted on the tunnel wall, provided remotely controlled longitudinal motion for the model. The pressure probes, being mounted on the permanent tunnel sting support system, were thus capable of remotely controlled longitudinal and lateral movement.

The test setup resembles that used in earlier sonic-boom testing (for example, ref. 1) with two exceptions. The models were offset from the actuator sting center line by a strut to prevent the strong actuator sting shock from interfering with the model shock system. In addition, the pressure probe strut was constructed in such a manner that for the high Mach numbers of this test, the complete pressure signature of the model could be registered by the measuring probe before the shocks impinged on the orifices of the reference probe.

The probes were very slender cones (2° cone half-angle), each having four 0.089-cm-diameter (0.035-in.) static-pressure orifices leading to a common chamber. Orifices were circumferentially spaced 90° apart and were arranged to lie in a Mach 2.92 plane originating at the model.

Although Mach 2.92 is at the low end of the range of this test, the Mach angle decreases by only about 7.5° to Mach 4.63. Earlier tests (ref. 1) over a greater range of Mach angles did not reveal any significant effect of a difference between the Mach angle and the orifice angle, and it is believed that no significant effect was present for this test.

4

Estimates were made of the possible error introduced through the use of the 2^0 half-angle-cone measuring probes. The maximum estimated error is on the order of 5 percent and occurs at Mach number 4.63 in the vicinity of the maximum measured overpressure. This error introduced by the measuring system yields a pressure rise slightly higher than that which actually occurs.

The investigation was conducted in the Langley Unitary Plan wind tunnel at Mach numbers of 2.96, 3.83, and 4.63, with stagnation pressures of 0.1379 MN/m^2 (20 psia), 0.206 MN/m^2 (30 psia), and 0.413 MN/m^2 (60 psia), respectively, and a stagnation temperature of 71.1^0 C (150^0 F). Because of the small Mach angle associated with Mach number 4.63 and the size of the tunnel test rhombus, the maximum lateral displacement which could be achieved between model and measuring probe was 25.4 cm (10 in.).

For this series of tests, the models were tested at three Mach numbers at a lateral displacement of 25.4 cm (10 in.). In addition, at Mach number 4.63, the models were tested at lateral displacements of 10.16 cm (4 in.) and 17.78 cm (7 in.).

THEORETICAL CONSIDERATIONS

The theoretical method of determining pressure fields about bodies of revolution at supersonic speeds (ref. 3) and the application of this method (described in refs. 4 and 5) was utilized to determine the theoretical sonic-boom signatures of the models. The method is based on a modified linearized theory where the linear characteristics are replaced by curved characteristics more closely approximating the real flow.

The function $F(\tau)$ used within the computer program to estimate the pressure signature is determined through application of Whitham's smooth-body equation

$$F(\tau) = \frac{1}{2\pi} \int_0^\tau \frac{A''(t)}{\sqrt{\tau - t}} dt$$

The area distribution used within this equation is obtained by passing a series of Mach planes oriented as shown in figure 3 through the configuration along the longitudinal axis of the model. The projections on the YZ-plane of the areas intercepted by the Mach planes establish an equivalent body of revolution which is one of a series of equivalent bodies of revolution used to estimate supersonic wave drag as described in reference 6.

Lomax has shown, in reference 7, that the wave drag of a configuration consists of the wave drag of a series of equivalent bodies of revolution due to volume and the wave drag of a series of equivalent bodies of revolution due to lift. The latter term is evaluated by determining the net force normal to the free stream due to surface pressures around the Mach-plane—configuration intersection. As is the case for the equivalent

bodies due to volume, an equivalent body due to lift is established for each orientation of the Mach planes about the longitudinal axis.

Calculation of the equivalent body of revolution due to lift by this method requires a knowledge of the detailed pressure distribution over the surface of the configuration at any desired angle of attack. Because such data is not readily available, it is customary to assume that the lift forces act at the mean camber plane and the effect of thickness on the equivalent bodies due to lift can be ignored both for wave drag (ref. 8) and for sonic boom (ref. 9). It will be shown in the section of this paper on the evaluation of the oblique forces that the effect of integrating the surface pressures along the Mach-plane— configuration intersection for establishing the equivalent body due to lift can be significant, particularly as the Mach number is increased.

However, most of the estimated sonic-boom pressure signatures of this paper use only the equivalent body of revolution due to volume for calculating the Whitham $F(\tau)$ function.

The Mach number range of the tests reported herein is for the most part above a Mach number of 3.0 which is generally regarded as an upper limit for linearized theory and where higher order effects may become significant. These effects can arise both from the nonlinear terms neglected in the development of the linearized supersonic flow equation and from the terms containing higher order powers and derivatives of $A'(t)$ which were neglected in the slender-body derivation of a source distribution for use in the Whitham function. For bodies of revolution with blunt noses, the assumption of small body angle with respect to the Mach angle is violated for all supersonic Mach numbers; however, for the blunt bodies of this investigation, the effects are localized at the nose and do not substantially affect the validity of the whole signature.

A typical model and its Mach-sliced area distribution used as input to the smooth body theoretical program is shown in the upper half of figure 3. A typical pressure signature identified as "Program output" is also shown in figure 3. The small-magnitude shocks occurring throughout the signature are the result of a loss of significant decimal places in the calculation of the area development and the calculation of the Whitham function $F(\tau)$ utilized in the determination of the pressure signature. These pseudoshocks have been smoothed out in the theoretical data presented in this report as shown in the sketch identified as "Faired signature" in figure 3. In fairing these curves, care was taken to preserve the maximum overpressure as well as the area under the positive part of the pressure signature. This latter feature of the pressure signature is defined as the signature impulse and is proportional to the energy imparted to the flow field by the disturbing body.

Another assumption of the smooth-body theory is that the first derivative of the area distribution be continuous. The computer program uses curve-fitting techniques

6

and fairs over the shoulder discontinuity of the models in this paper. However, the rate of change of area in the vicinity of the shoulder is still sufficiently large that a strong trailing shock is predicted.

A more rigorous solution from reference 3 for nonsmooth bodies of revolution utilizes the Stieltjes integral for evaluation of the F function. This solution, which is the basis for a nonsmooth-body method for evaluation of pressure signatures, has been found to yield a more accurate prediction of the signature in the vicinity of a discontinuity. Unlike the smooth-body theory, this solution starts the disturbances at the body surface rather than along the longitudinal axis, and therefore finds application only to configurations which can, with little distortion, be represented as bodies of revolution.

RESULTS AND DISCUSSION

Smooth-Body Theory

The experimental pressure distributions for all the models at zero angle of attack and a lateral distance from the model of 25.4 cm (10 in.) are shown in figure 4. Theoretical pressure distributions, obtained by using smooth-body theory, are also shown. The data are grouped by body shape and are plotted in a parametric form which is standard for this type of presentation. The significance of the parameters, from theoretical considerations, is that once the lateral distance from the model is sufficient for the pressure signature to attain the characteristic far-field N-wave shape, the signature in parametric form for steady-flight conditions does not change, regardless of further increase in distance from the model.

The experimental pressure signatures do not exhibit a step increase in pressure across the shock waves, but rather a gradual rise in pressure where the shock is first encountered by the measuring probe, followed by a rapid pressure rise, and then a rounding-off of the pressure peak. The reason for the lack of sharply defined shocks in the experimental data is discussed in detail in reference 5 and is primarily due to vibration of the model and measuring probe in the wind tunnel.

A significant difference can be observed, for the cone models in particular, between the experimental and theoretical shapes of the expansion portion of the pressure signature following the bow shock. Although the theoretical slope is independent of the configuration, the slope of the experimental data increases as the model size increases. It appears that for the signatures with near-field properties which are generally associated with the more slender bodies, the theoretical and experimental expansion slopes agree but as the signatures assume the far-field N-wave shape, the expansion shown by the experimental data is more rapid than that predicted by theory. For this paper, the theoretical signature is considered to be far field when the bow-shock jump is followed by a linear expansion through the reference axis; thus, the forward part of an N-wave is formed.

Because of the lack of a sharply defined starting position of the bow shock on the measured pressure signature, the theoretical signature is arbitrarily alined with the measured signature at the point where the expansion part of the signature intercepts the horizontal axis. In the theoretical analysis, this point corresponds to the F function passing through zero. Large differences between the measured and theoretical signatures in the expansion region of the signature (for instance, the cone signatures at high Mach numbers) suggest that some contributions to the area distribution from which the F function is derived may have been neglected. Factors which modify the area distribution and thus the theoretical signature are discussed in a later section.

In general, the behavior of the theoretical signatures and the measured signatures is much as would be expected; that is, the bow-shock strength and the length of the signature tend to increase with increasing Mach number, as well as with decreasing fineness ratio of the forebody. Another characteristic of both the theoretical and measured signatures is that as the Mach number is increased, the positive part of the signature tends more toward the characteristic far-field N-wave shape. This condition is particularly true for the models with conical forebodies, where at M = 4.63, even the most slender model produces an essentially far-field signature.

A comparison between the measured and predicted maximum overpressures for $h/l = 5$ is shown in figure 5. The data are plotted as a function of bluntness parameter n and grouped according to fineness ratio and Mach number. The tendency for the predicted overpressure to be higher than the measured overpressures can be attributed to the rounding of the pressure peaks in the measured signatures. As a function of bluntness parameter n, the lowest predicted maximum overpressures occur for the linear area bodies (n = 0.5) and this trend is verified by the experimental data.

In figure 6, a comparison between experimental and predicted signature impulse is shown. The impulse should be independent of probe and model vibration and thus should provide a good indication of the adequacy of the theoretical method. Although the theory does show the trend toward increased impulse with increasing model size and increasing Mach number, it grossly underpredicts the impulse for several cases, particularly for the blunt bodies at the higher Mach numbers. However, as will be shown later, the addition of a boundary layer to the model area distribution used for the theoretical prediction results in a significant increase in signature impulse and improves the agreement with experiment. It should be noted that an increase in the predicted impulse is necessarily accompanied by an increase in maximum overpressure; thus, the correlation shown in figure 5 would be adversely affected.

Theoretical and measured pressure signatures for a Mach number of 4.63 and various perpendicular distances from the models are shown in figure 7. Because of the size

of the tunnel, the perpendicular distance range is small, from 2 to 5 body lengths; and as a consequence, there are only small variations between the signature measured closest to the model and that measured farthest from it.

The maximum overpressure parameter and the signature impulse parameter as a function of perpendicular distance are summarized in figures 8 and 9. Much the same conclusions can be stated regarding the correlation between theory and experiment as for the signatures of figure 4.

The maximum overpressure parameter is predicted reasonably well, with the exception of the largest of the blunt forebody shapes. The correlation between theoretical and experimental signature impulse is poor, however, and is especially poor for the blunt forebody models.

A summary of the data presented thus far is shown in figure 10. The degree to which the theory underpredicts the signature impulse parameter is easily seen in this figure. The poorest correlation is generally associated with the blunt forebody shape. Models 1, 2, and 3 are identical to models 1, 4, and 5, respectively, of reference 1 which included data for Mach numbers from 1.26 to 2.01. In order to show the variation of the predicted and measured signatures over a greater range of Mach numbers, the data from reference 1 for Mach number 1.41 at an h/l value of 5 are shown in figure 11 with the signatures for Mach numbers of 2.96 and 4.63. It should be pointed out that the data of reference 1 were obtained in the Langley 4-foot supersonic pressure tunnel under somewhat different test conditions. However, the data-reduction techniques eliminate most of these variables so that, for purposes of this paper, a valid comparison may be made.

The agreement between theory and experiment which is excellent at $M = 1.41$ decreases with increasing Mach number, particularly for the blunt forebody model 3. The increase in maximum overpressure and signature length for the higher Mach numbers is particularly noticeable when compared with the data for Mach 1.41.

The signature impulse from reference 1 for Mach 1.41 compared with the data from the higher Mach numbers is shown in figure 12. Model 1 is a very slender cone with a half-angle considerably less than the Mach angle, even at Mach 4.63. As a consequence, the assumptions of linear theory more realistically apply to this model and as can be seen, the theoretical signature impulse closely follows the measured values.

Although the rapid increase of signature impulse with increasing Mach number for all three body shapes indicates the importance of sonic boom for configurations operating in the low hypersonic speed range, the higher operating altitudes for such aircraft will be a factor in attenuating the maximum overpressures propagating to the ground.

Addition of Oblique Force Term

As mentioned earlier, Lomax has shown that the wave drag of a configuration is composed of a volume term and a lift term. For a body of revolution at zero angle of attack, the wave drag due to lift is zero; however, the equivalent body of revolution due to lift for any single orientation of the Mach planes is not zero as shown in figure 13.

The cone model shown has a surface pressure distribution which consists of a constant positive pressure over the conical forebody, an expansion at the shoulder and an inverse square root decay along the cylindrical section of the model. If, for example, a Mach plane is passed through the model so that it intersects the model XY-plane at the shoulder, the result of integrating the Z-component of the pressure over the cone-plane intersection will be a net force per unit length in the negative Z-direction, and the result of integrating the Z-component of the pressure over the cylinder-plane intersection will be a net force per unit length also in the negative Z-direction. For a series of cutting planes along the longitudinal axis, a distribution of this force per unit length (ΔL) is calculated and is shown in figure 13. The equivalent body of revolution B(t) is obtained by a summation along the longitudinal axis. The distribution of the oblique force is referred to as a lift distribution because it corresponds to the lift distribution used in calculating the sonic-boom characteristics of a conventional winged configuration.

The effect of the lift term on the theoretical prediction of the pressure signature is shown in figure 14. A conical forebody model was chosen because of its known surface pressure distribution and because it somewhat simplified the analysis. Equivalent area distributions for two Mach numbers are shown as well as the experimental and theoretical pressure signatures.

As might be expected from examination of the B(t) area distributions, the greatest effect of the lift component is on the aft part of the pressure signature. For the $M = 2.96$ signature, the aft part is considerably improved with the addition of lift, and closely approximates the measured signature. For the $M = 4.63$ signature, the effect of the lift term is to reduce the length of the signature and the strength of the trailing shock; however, the theoretical signature still varies considerably from the measured signature. It should be noted that the theoretical signatures were alined along the linear expansion parts of the experimental signature rather than at the horizontal-axis intersection.

It was suggested earlier that some contributions to the area distribution for the F function calculation in the expansion part of the signature may have been neglected. Comparison of the two theoretical signatures with the experimental data indicates that the addition of the lift term provides a better definition of the equivalent-area distribution in this region.

Nonsmooth-Body Theory and Boundary Layer

Because of the poor correlation between experiment and smooth-body theory in the region of the trailing shock, a signature was calculated by using nonsmooth-body theory for the largest of the cone bodies (model 7).

A comparison is shown in the upper half of figure 15 of signatures calculated by using the nonsmooth-body theory and the smooth-body theory with lift. The nonsmooth-body theory predicts more accurately the trailing portion of the signature in the region affected by the shoulder discontinuity; however, because of limitations of the computer program numerical techniques, a lower peak overpressure and consequently less impulse are predicted than for the smooth-body theory. It should be noted that for supersonic Mach numbers below the range of this investigation, the nonsmooth-body theory estimates of the bow shock part of the signature correspond more closely to the estimates of smooth-body theory. (See ref. 9.)

Another factor which affects the measured pressure signature in the wind tunnel is the relatively large boundary-layer displacement thickness on the model. The method of reference 10 was used to calculate the boundary-layer displacement thickness for model 7 and its effect on the predicted signatures is also shown in figure 15.

At a Mach number of 4.63, the inclusion of the boundary layer in the program has a significant effect on the entire theoretical signature. In particular, the signature impulse increases to approximate closely the experimental value. It would appear that consideration of the boundary layer is a requirement to increase the accuracy of predicting pressure signatures for the Mach number range of this report. However, because the boundary-layer displacement thickness is itself an estimate, it was included only in the predicted signatures of figure 15.

CONCLUDING REMARKS

A wind-tunnel investigation has been conducted at Mach numbers of 2.96, 3.83, and 4.63 of a series of bodies of revolution to determine the pressure signatures generated by the bodies. It was found that with minor modifications, test procedures which had been used in earlier tests at lower Mach numbers were adequate for the Mach number range of this test.

Although the size limitations of the test facility limited the maximum spacing between model and measuring probe to five body lengths, far-field pressure signatures were developed by several of the bodies. The data show that as Mach number increases, the far-field signature develops closer to the model.

A smooth-body theoretical method for predicting the pressure signatures which has given good correlation with experiment for low supersonic Mach numbers appears to be only qualitatively correct for the higher Mach numbers of this test. In general, the agreement between theory and experiment decreased with both increasing Mach number and decreasing model fineness ratio. In addition, the agreement between theory and experiment tended to decrease with increasing nose bluntness. The addition to the theoretical program inputs of a term analogous to a lift distribution improved the shape of the predicted signature and the addition of an estimated boundary layer improved the prediction of signature impulse. Estimation of the pressure signature using a nonsmooth-body method produced a better correlation for the trailing shock, but some reduction of the signature impulse.

Langley Research Center,
        National Aeronautics and Space Administration,
                Hampton, Va., February 8, 1971.

REFERENCES

1. Carlson, Harry W.; Mack, Robert J.; and Morris, Odell A.: A Wind-Tunnel Investigation of the Effect of Body Shape on Sonic-Boom Pressure Distributions. NASA TN D-3106, 1965.

2. Jones, L. B.: Lower Bounds for Sonic Bangs. J. R. A. S. (Tech. Notes), vol. 65, no. 606, June 1961, pp. 433-436.

3. Whitham, G. B.: The Flow Pattern of a Supersonic Projectile. Commun. Pure Appl. Math., vol. V, no. 3, Aug. 1952, pp. 301-348.

4. Middleton, Wilbur D.; and Carlson, Harry W.: A Numerical Method for Calculating Near-Field Sonic-Boom Pressure Signatures. NASA TN D-3082, 1965.

5. Carlson, Harry W.: Correlation of Sonic-Boom Theory With Wind-Tunnel and Flight Measurements. NASA TR R-213, 1964.

6. Harris, Roy B., Jr.: An Analysis and Correlation of Aircraft Wave Drag. NASA TM X-947, 1964.

7. Lomax, Harvard: The Wave Drag of Arbitrary Configurations in Linearized Flow as Determined by Areas and Forces in Oblique Planes. NACA RM A55A18, 1955.

8. Harris, Roy V., Jr.: A Numerical Technique for Analysis of Wave Drag at Lifting Conditions. NASA TN D-3586, 1966.

9. Carlson, Harry W.; Mack, Robert J.; and Morris, Odell A.: Sonic-Boom Pressure Field Estimation Techniques. J. Acoust. Soc. Amer., vol. 39, no. 5, pt. 2, May 1966, pp. S10-S18.

10. Mirels, H.; and Ellinwood, John W.: Hypersonic Viscous Interaction Theory for Slender Axisymmetric Bodies. AIAA Pap. No. 68-1, Jan. 1968.

Model	k
1	.01
4	.02
7	.04

Equation

$$r = x \sqrt{\frac{k}{\pi}}$$

Conical forebody

Model	k
2	.02
5	.04
8	.08

$$r = x^{\frac{1}{2}} \sqrt{\frac{k}{\pi}}$$

Linear-area forebody

Model	k
3	.04
6	.08
9	.16

$$r = x^{\frac{1}{4}} \sqrt{\frac{k}{\pi \sqrt{2}}}$$

Blunt forebody

$l = 2$ in. (5.08 cm)
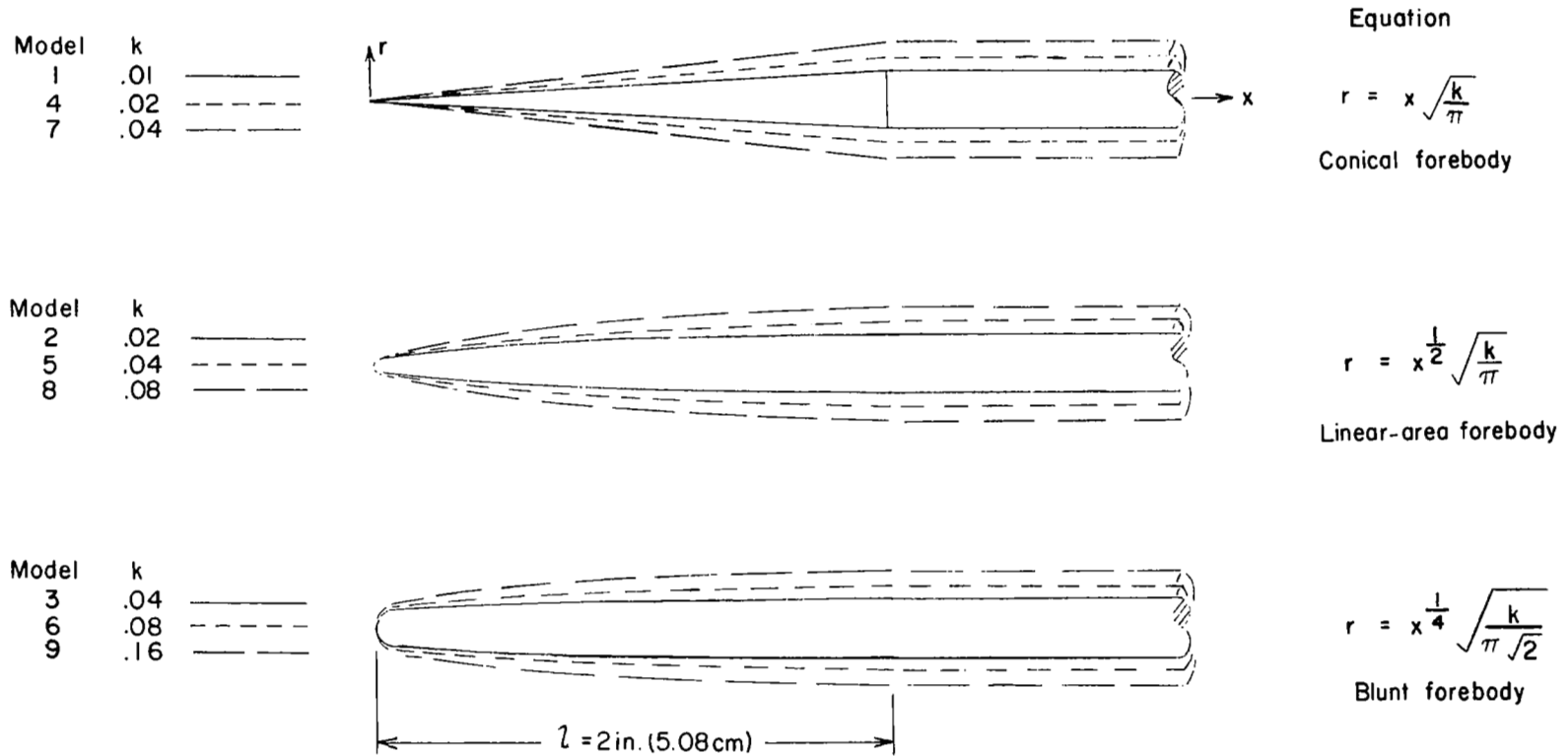
Figure 1.- Models with equations for model radii.
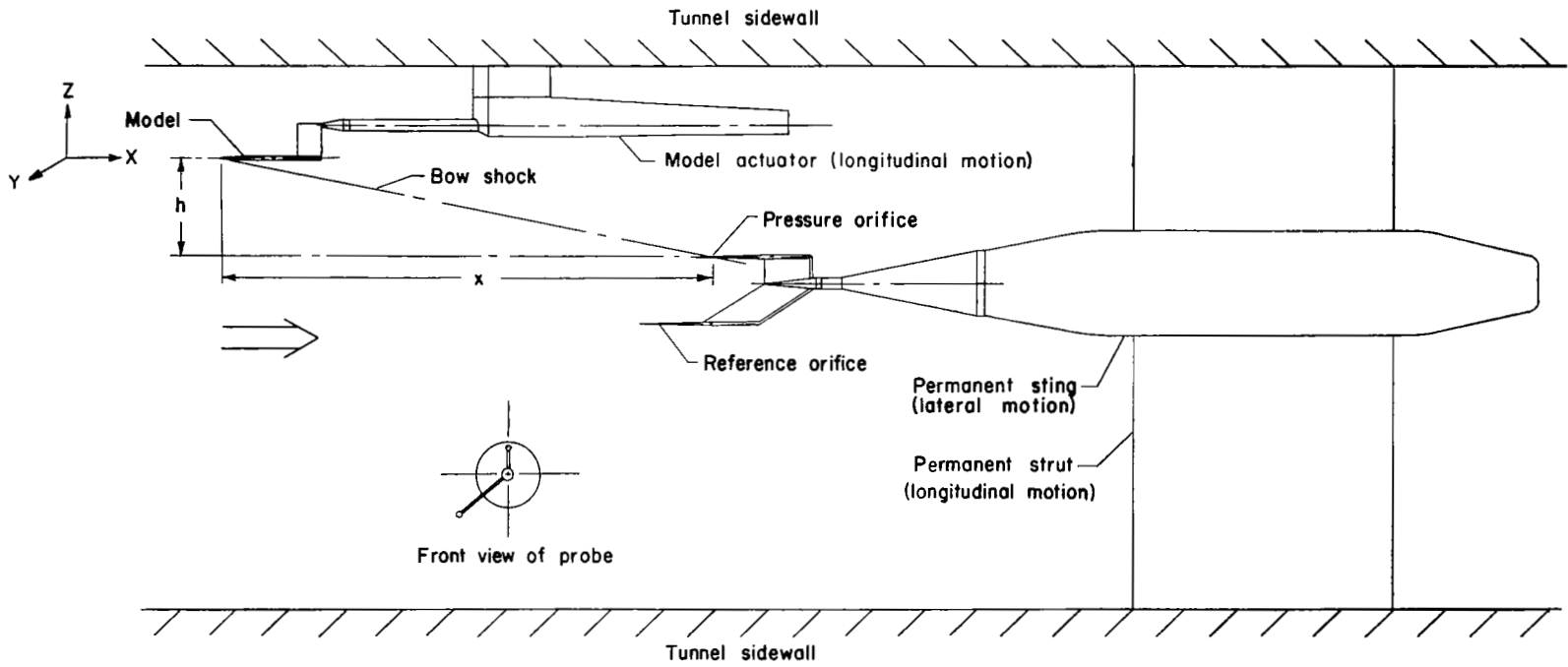
Figure 2.- Plan view sketch of wind-tunnel apparatus.
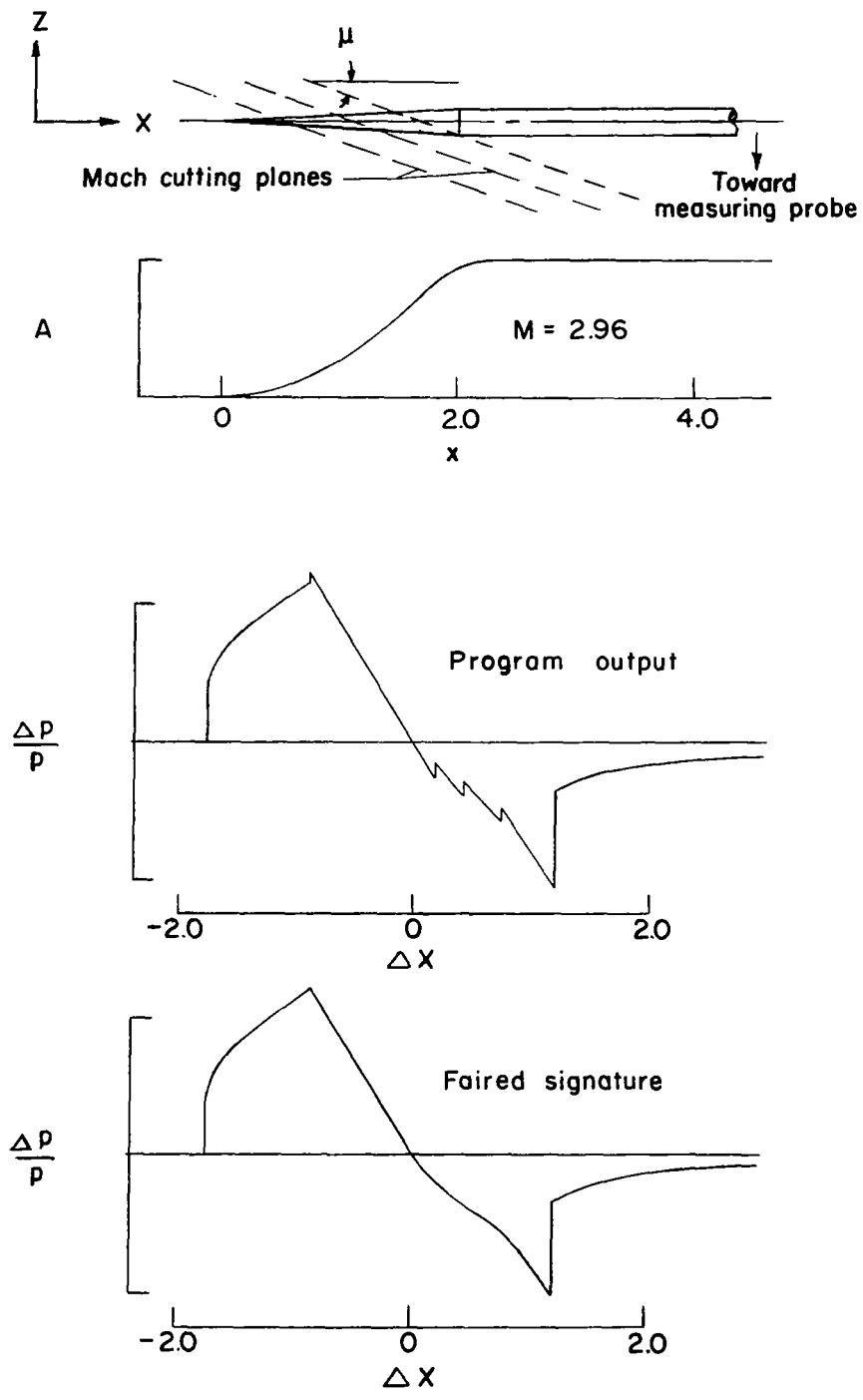
Figure 3.- Typical smooth-body program input and output.
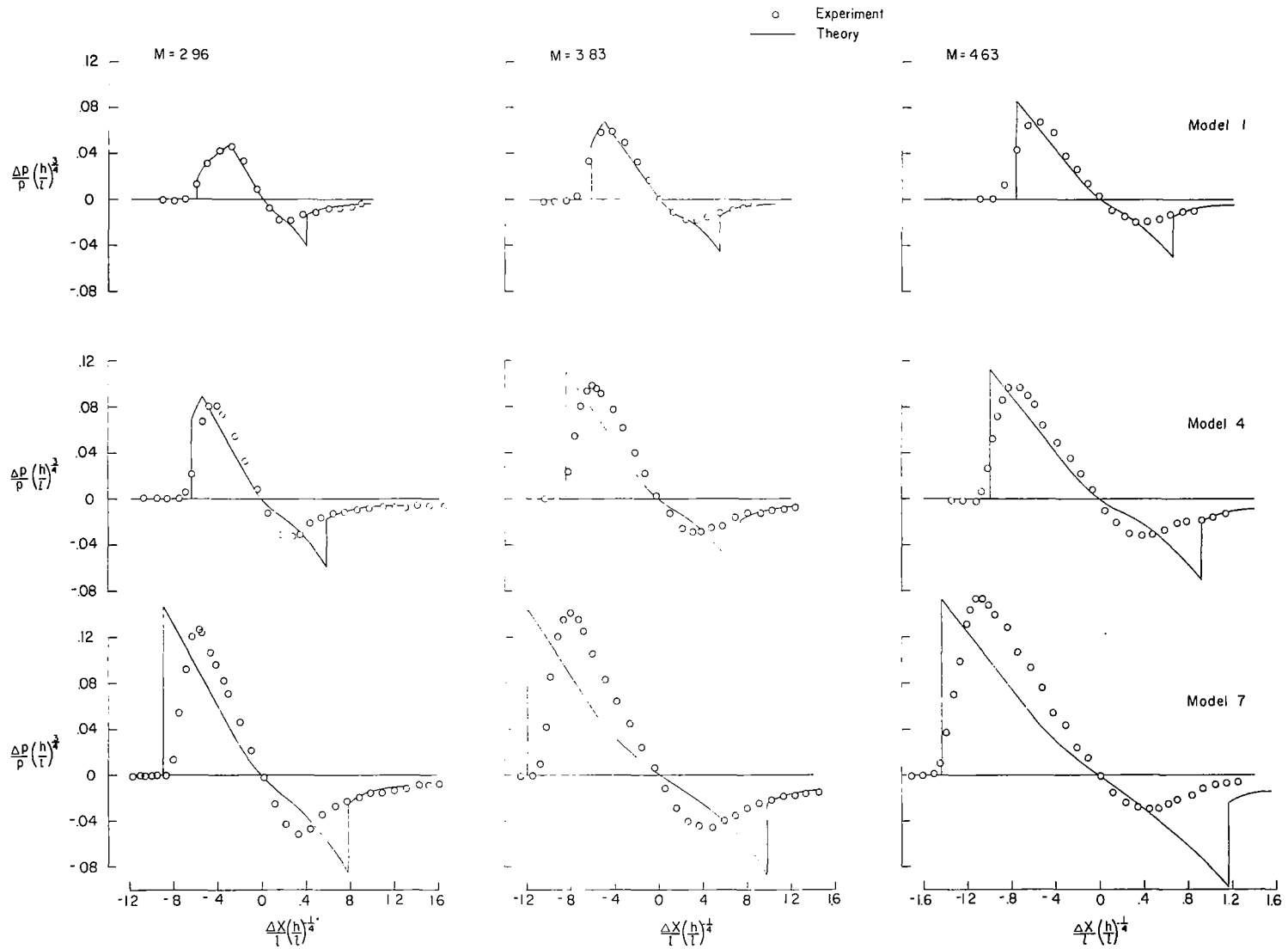
(a) Cone series; models 1, 4, and 7.

Figure 4.- Pressure distributions for the various models. $h/l = 5$.
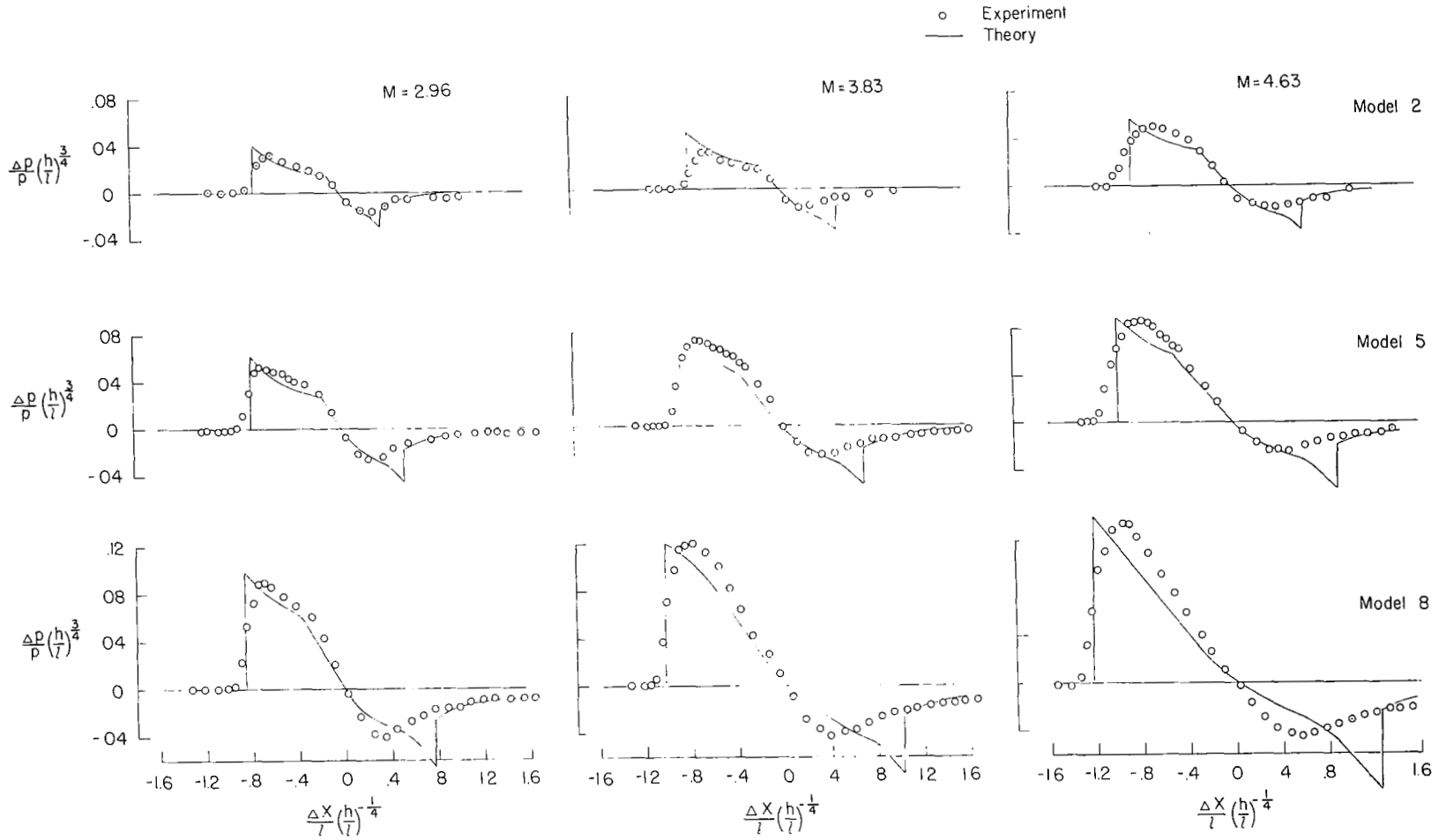
(b) Linear-area development series; models 2, 5, and 8.

Figure 4.- Continued.
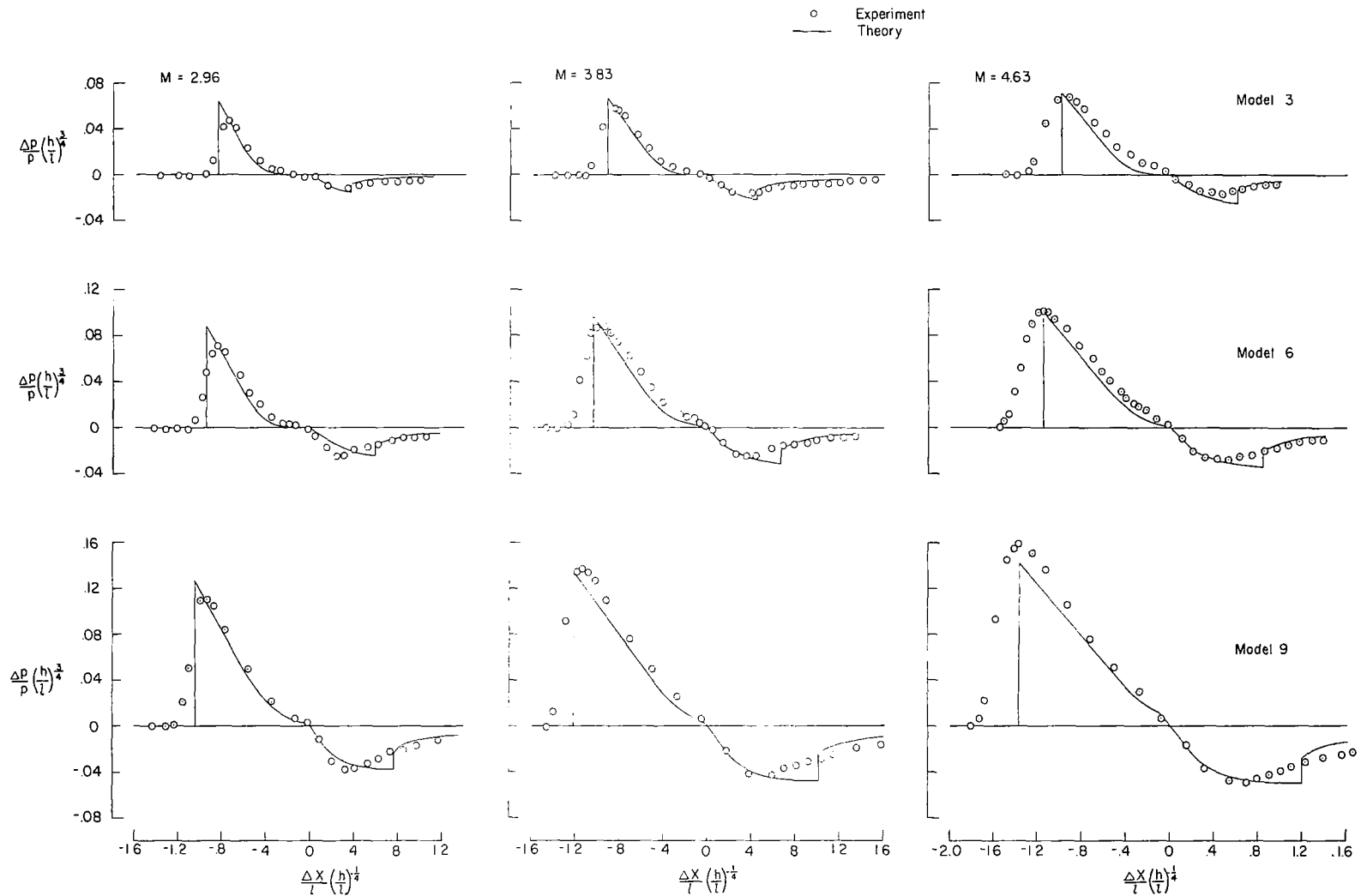
(c) Blunt series; models 3, 6, and 9.

Figure 4.- Concluded.
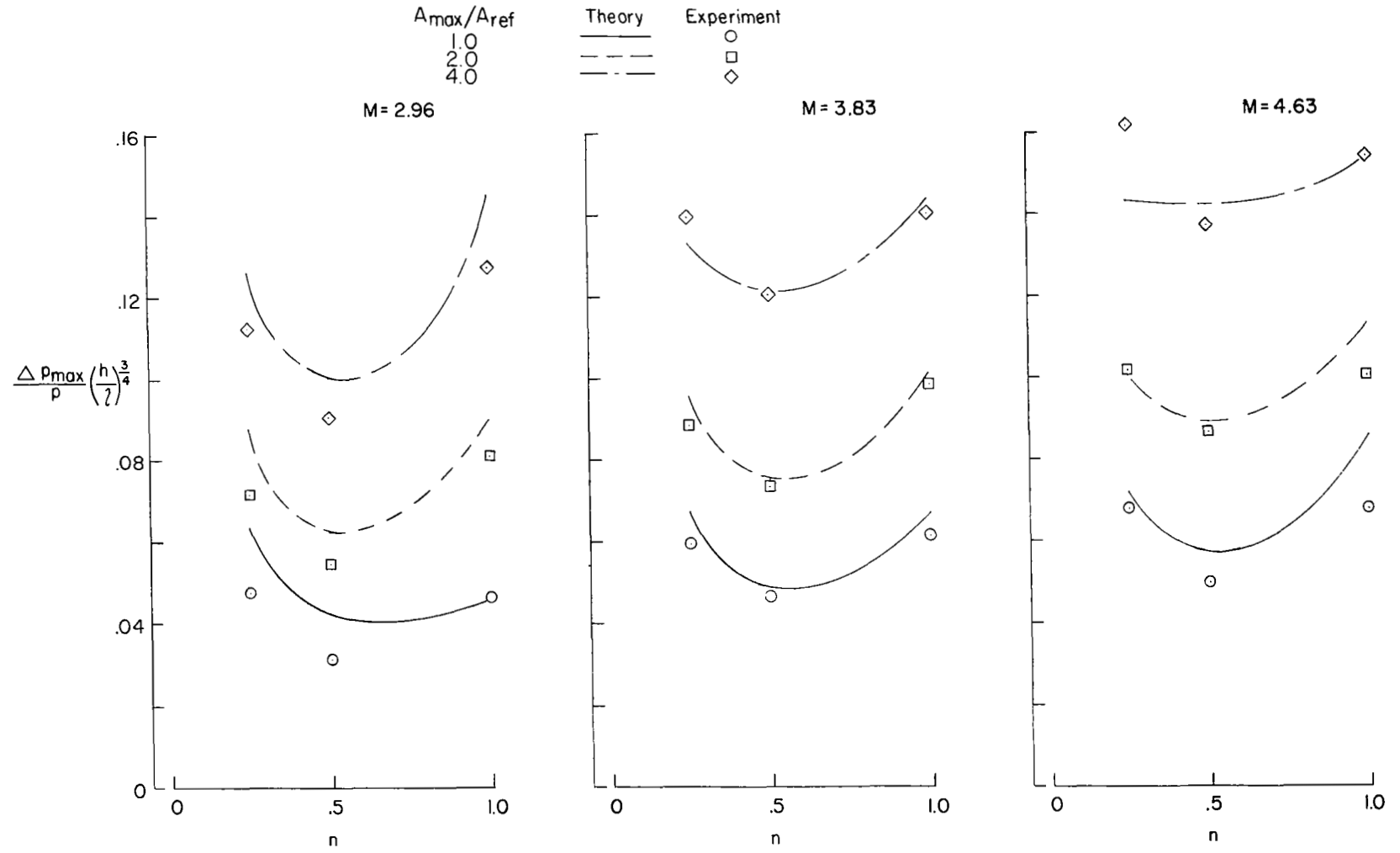
Figure 5.- Variation of maximum overpressure parameter with bluntness parameter. $h/\ell = 5.$

A_{max}/A_{ref} Theory   Experiment

1.0 ———— ○
2.0 ———— □
4.0 —·—·— ◇

.16

M = 2.96

.12

$\int \frac{\Delta p}{p} d\left(\frac{x}{l}\right)\left(\frac{h}{l}\right)^{\frac{1}{2}}$

.08

.04

0

0   .5   1.0

n

M = 3.83

0   .5   1.0

n

M = 4.63

0   .5   1.0

n
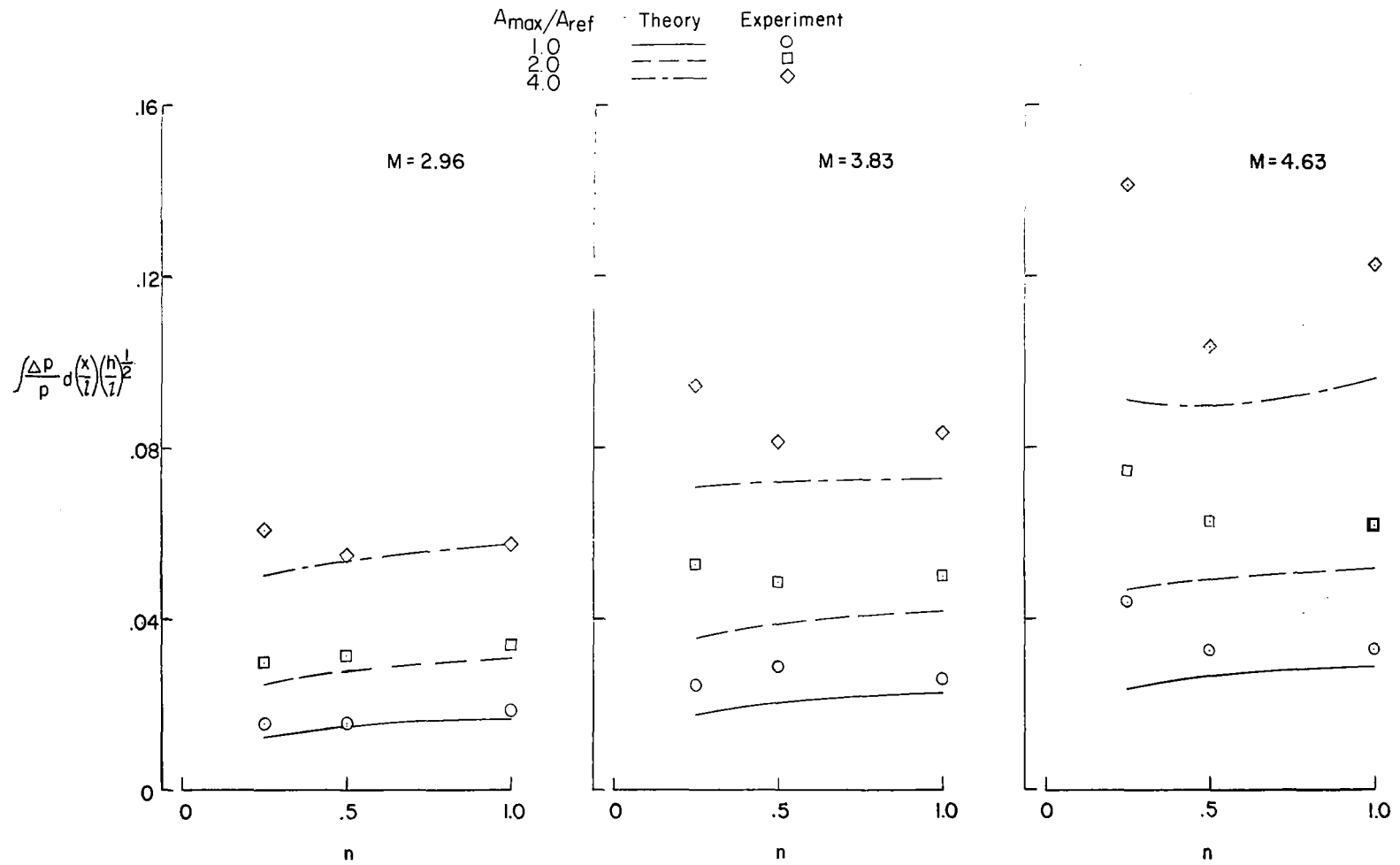
Figure 6.- Variation of signature impulse parameter with bluntness parameter.
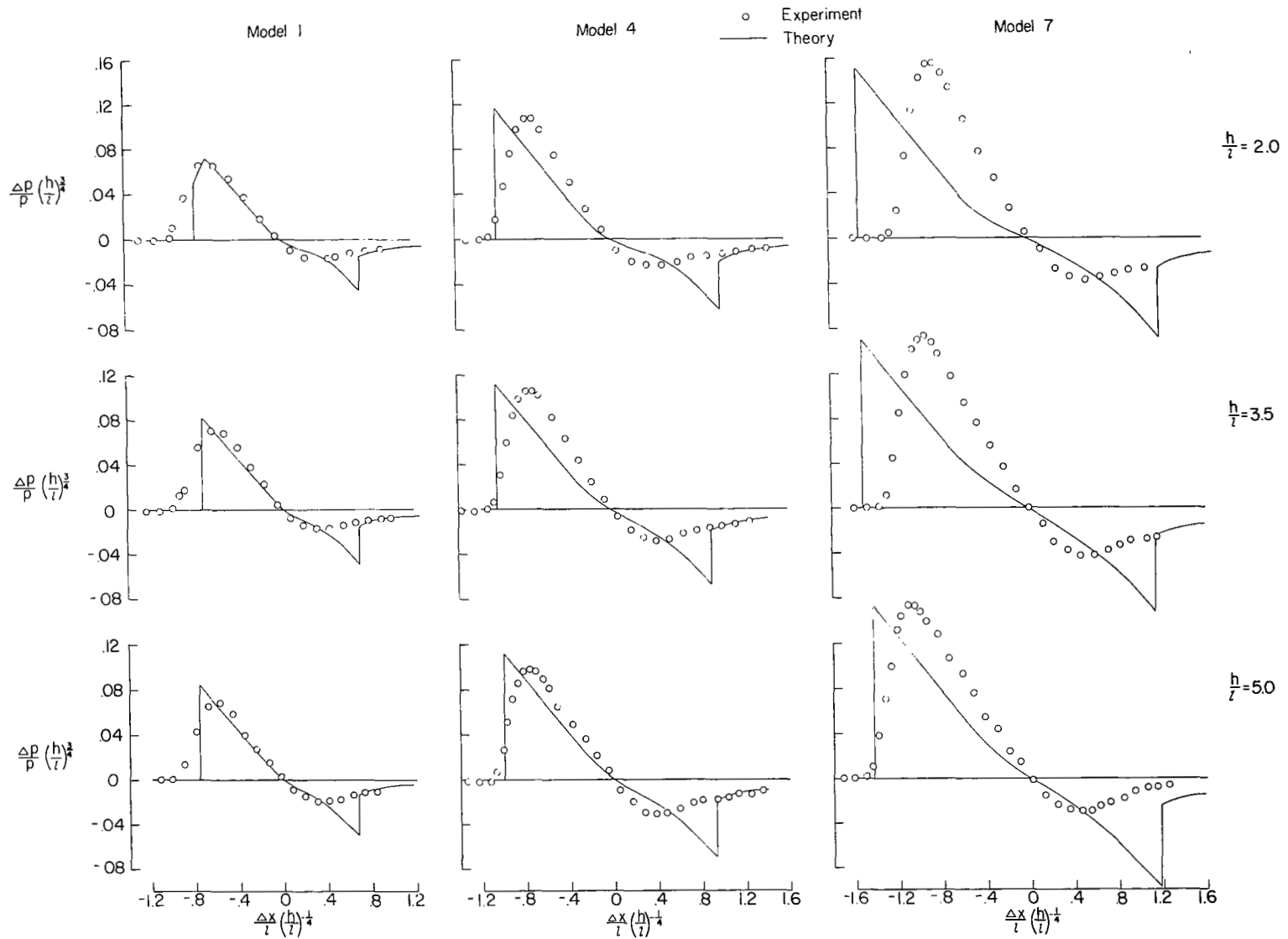
(a) Models 1, 4, and 7.

Figure 7.- Pressure distributions at various perpendicular distances. M = 4.63.
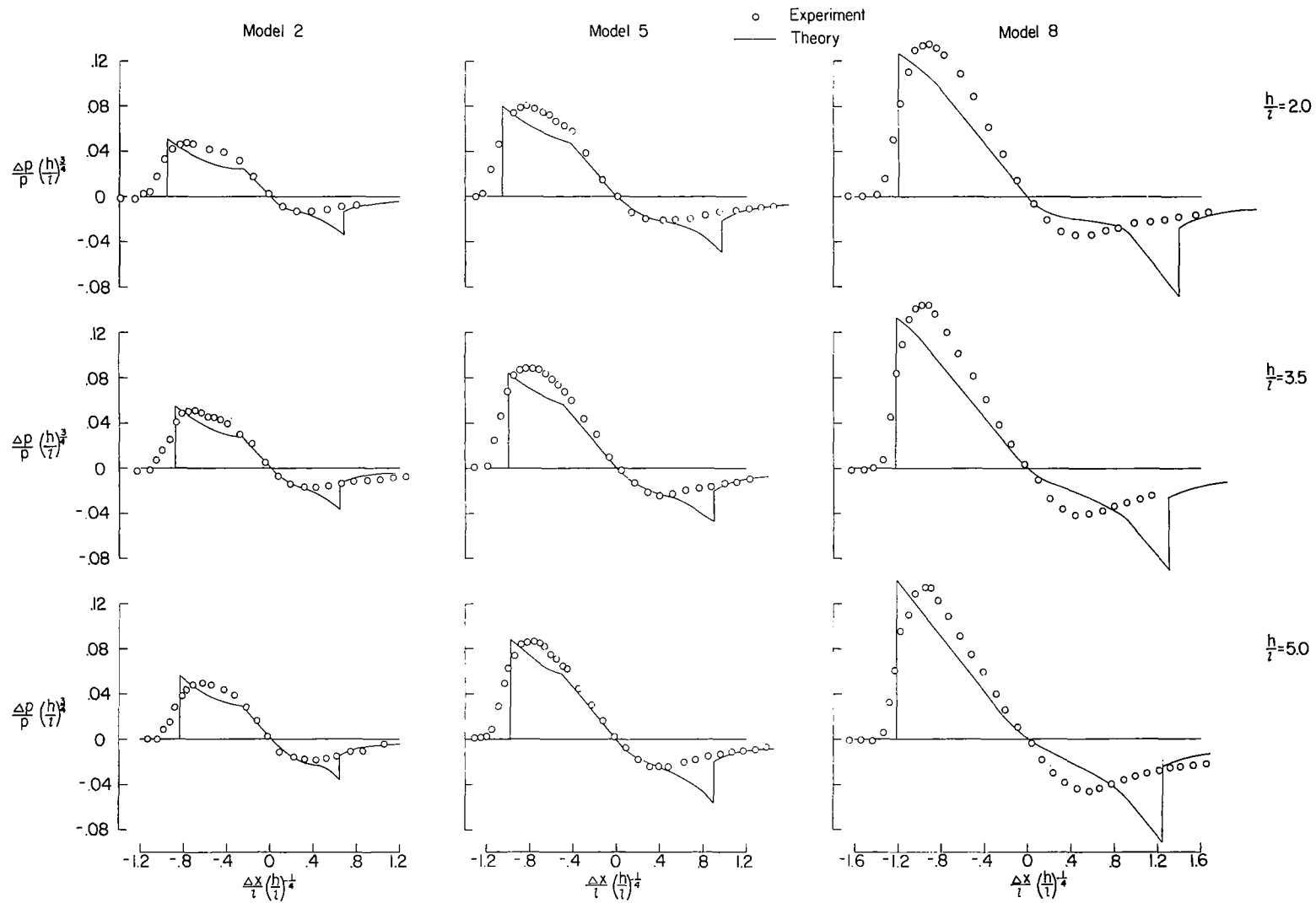
(b) Models 2, 5, and 8.

Figure 7.- Continued.
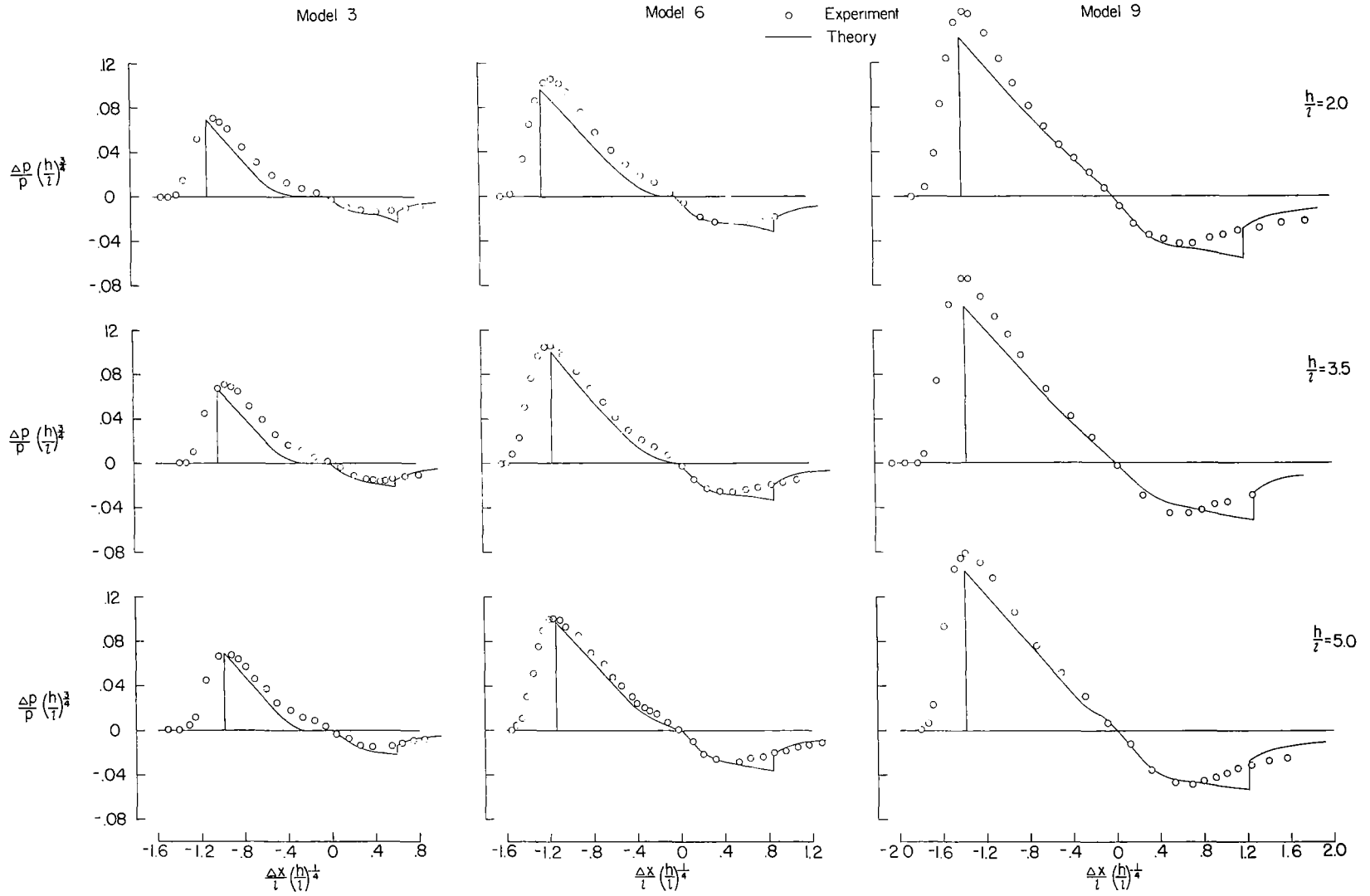
(c) Models 3, 6, and 9.

Figure 7.- Concluded.
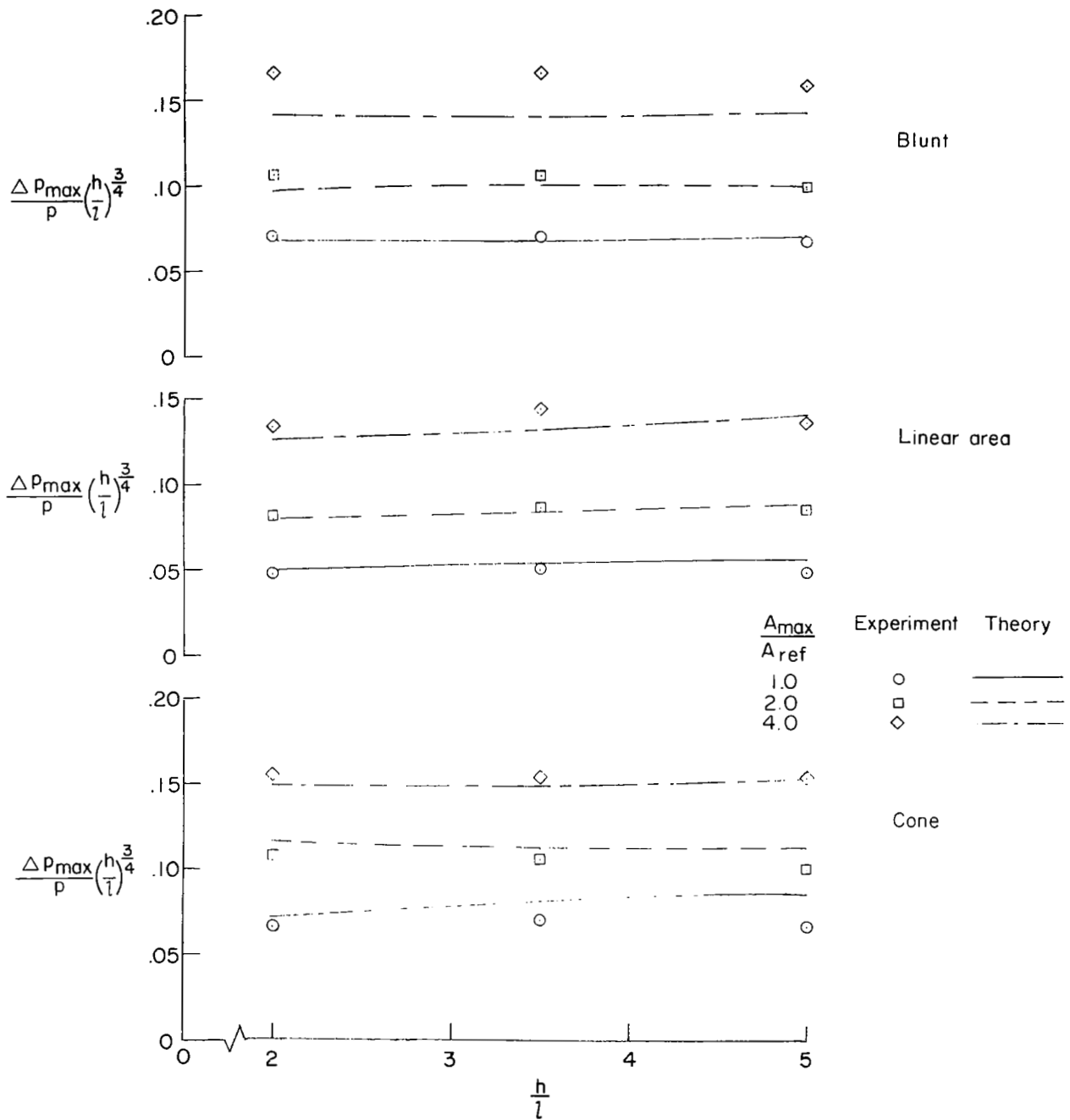
Figure 8.- Variation of maximum overpressure parameter with perpendicular distance.   M = 4.63.
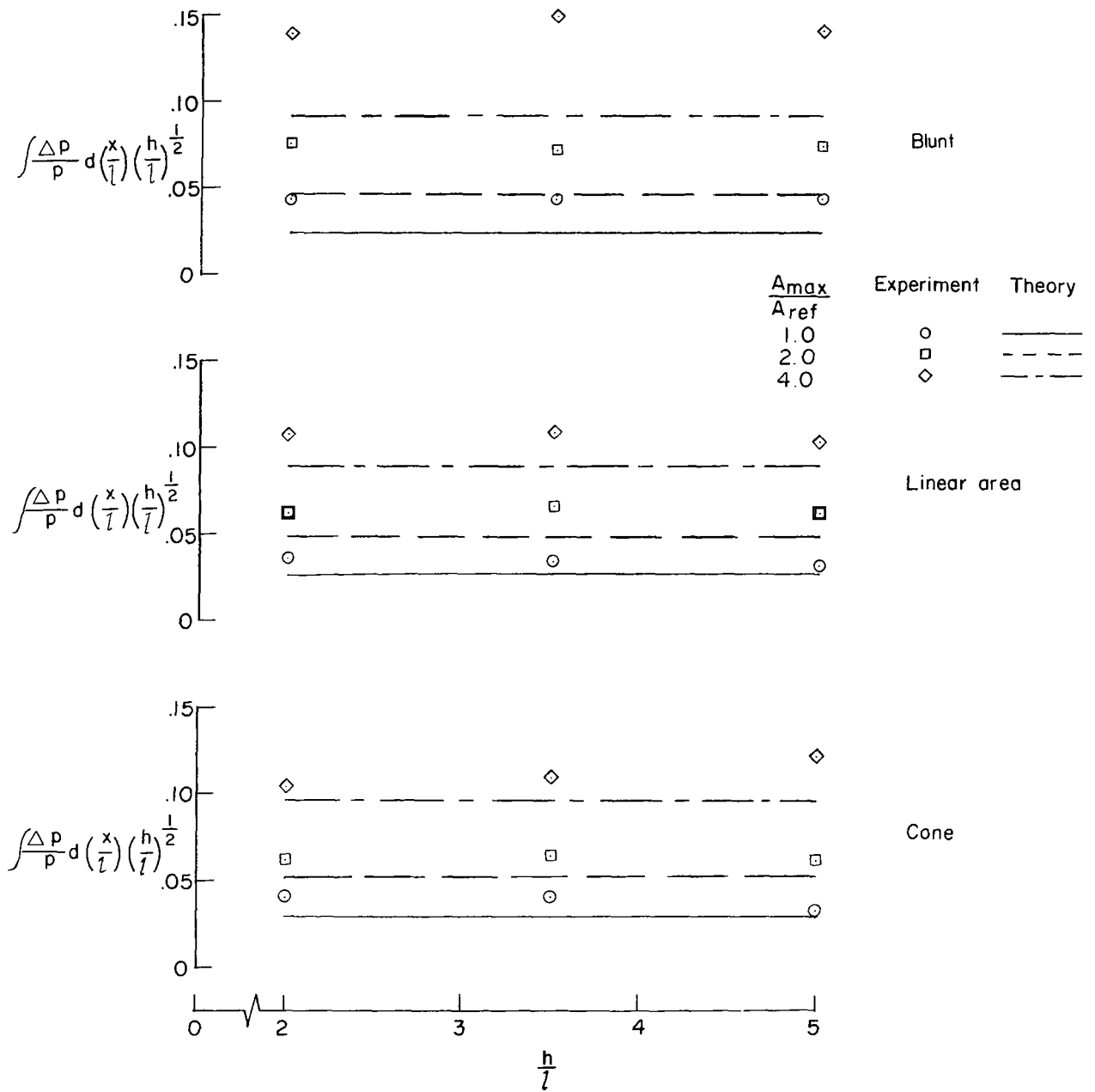
Figure 9.- Variation of signature impulse parameter with perpendicular distance. $M = 4.63$.
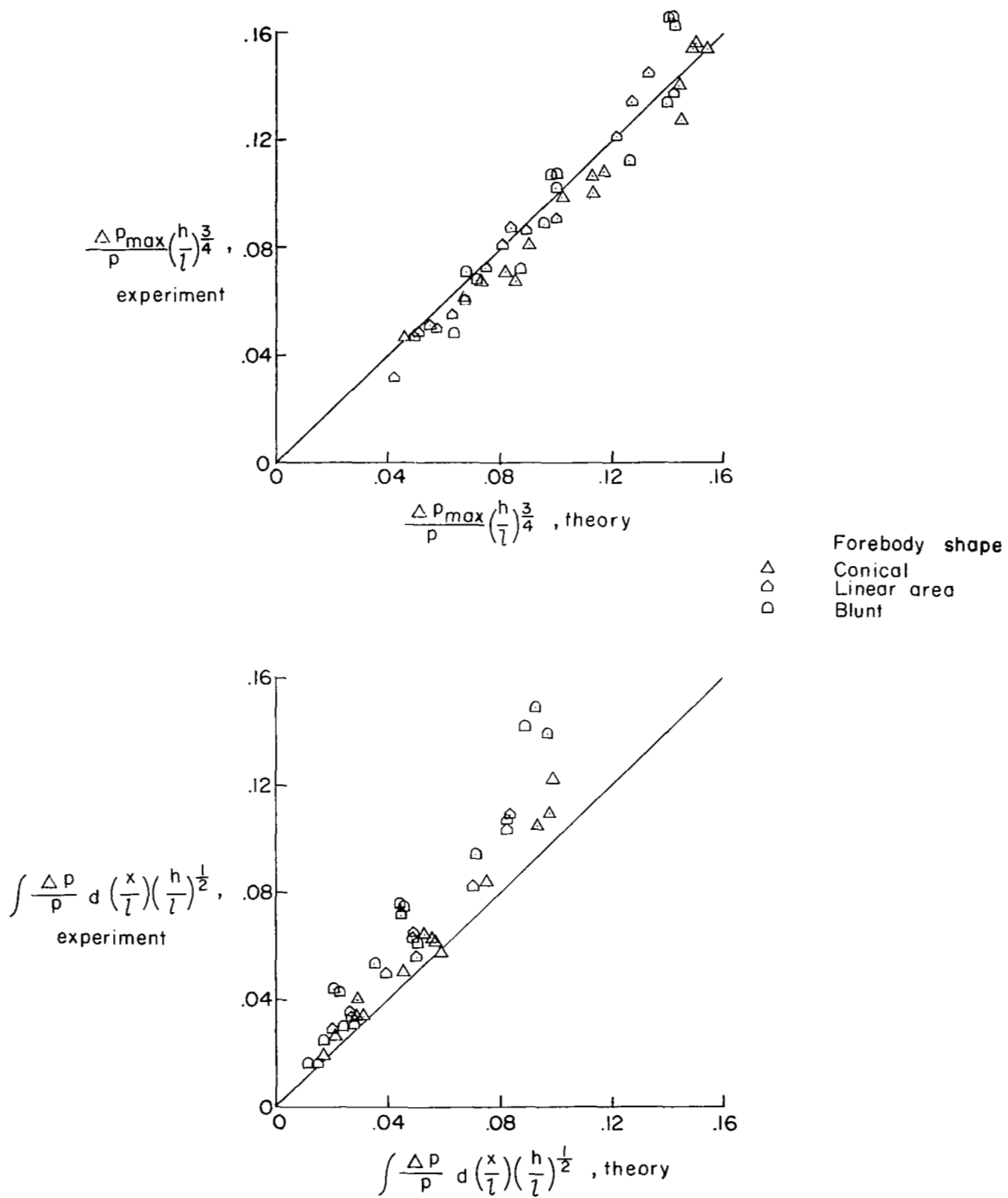
Figure 10.- Correlation of theoretical and experimental sonic-boom parameters.
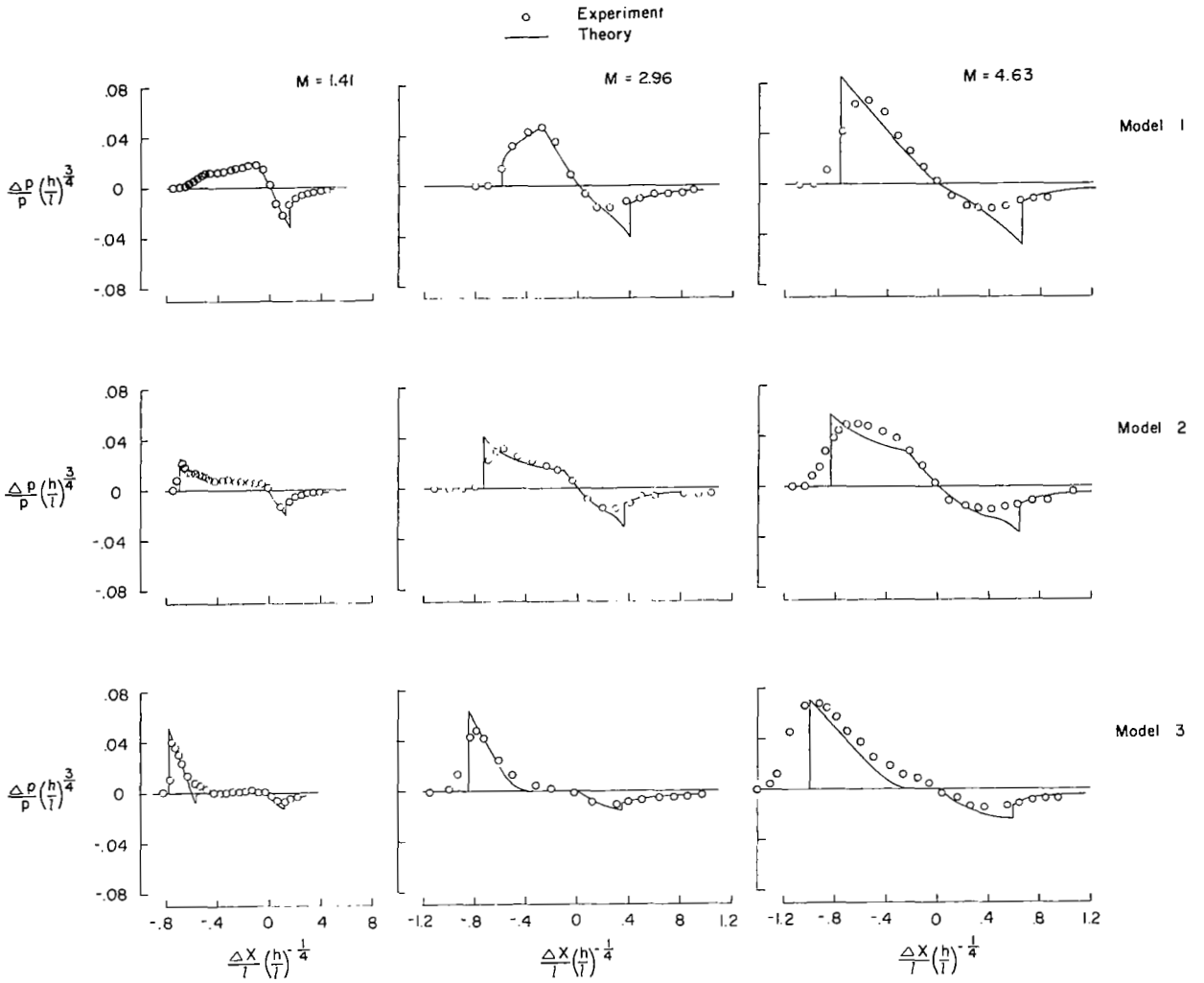
Figure 11.- Pressure distributions at $M = 1.41$, 2.96, and 4.63. $h/l = 5$. Data at $M = 1.41$ from reference 1.
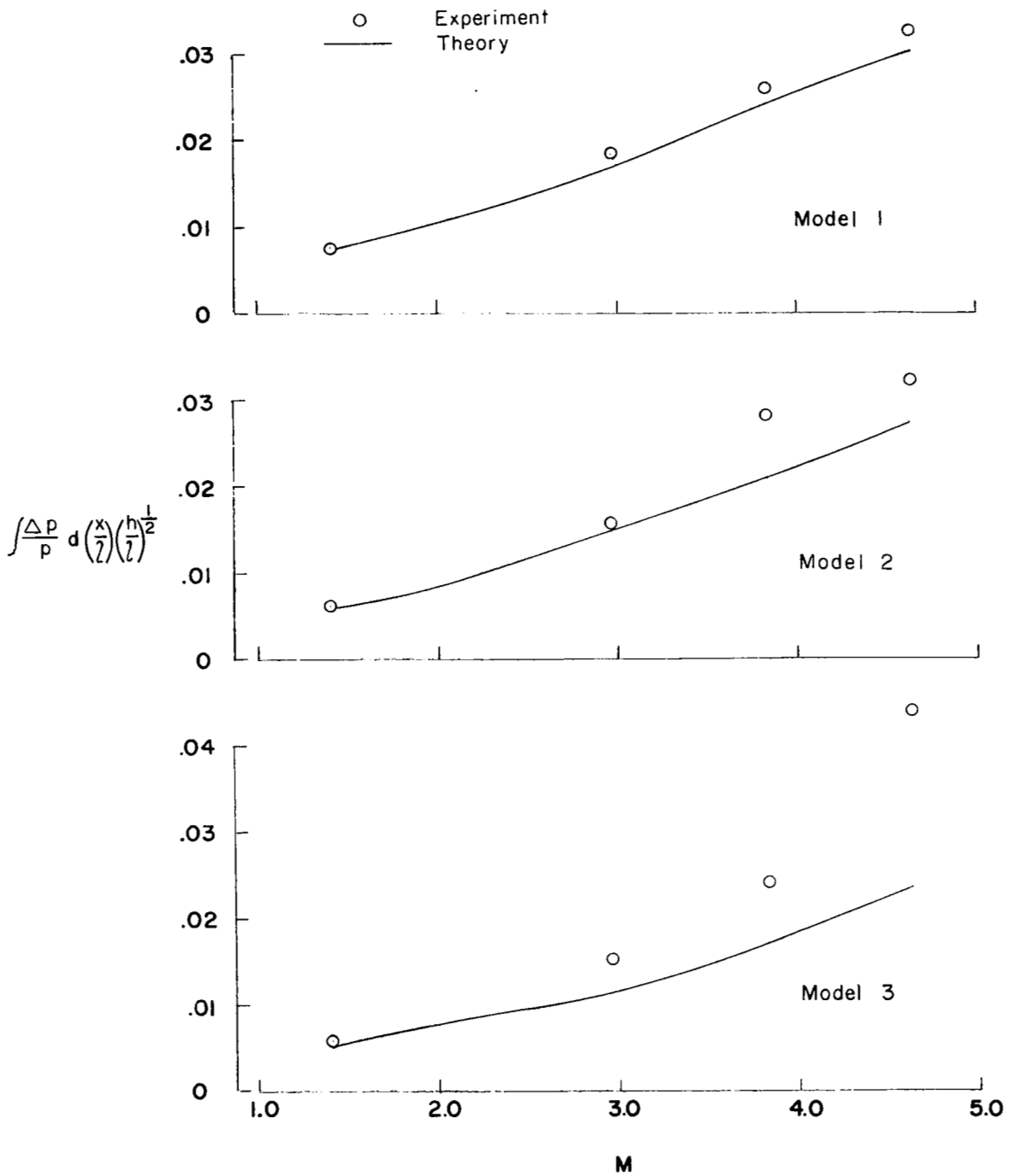
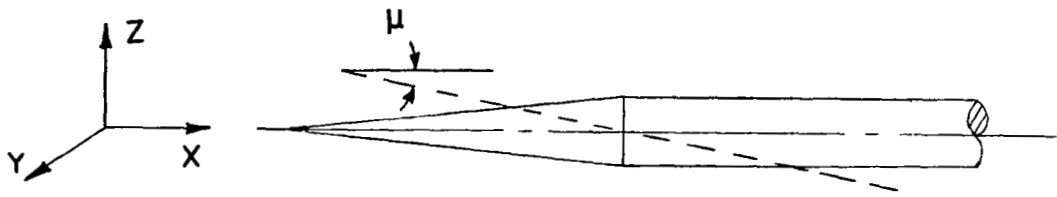Figure 12.- Variation of signature impulse parameter with Mach number. Data at M = 1.41 from reference 1.
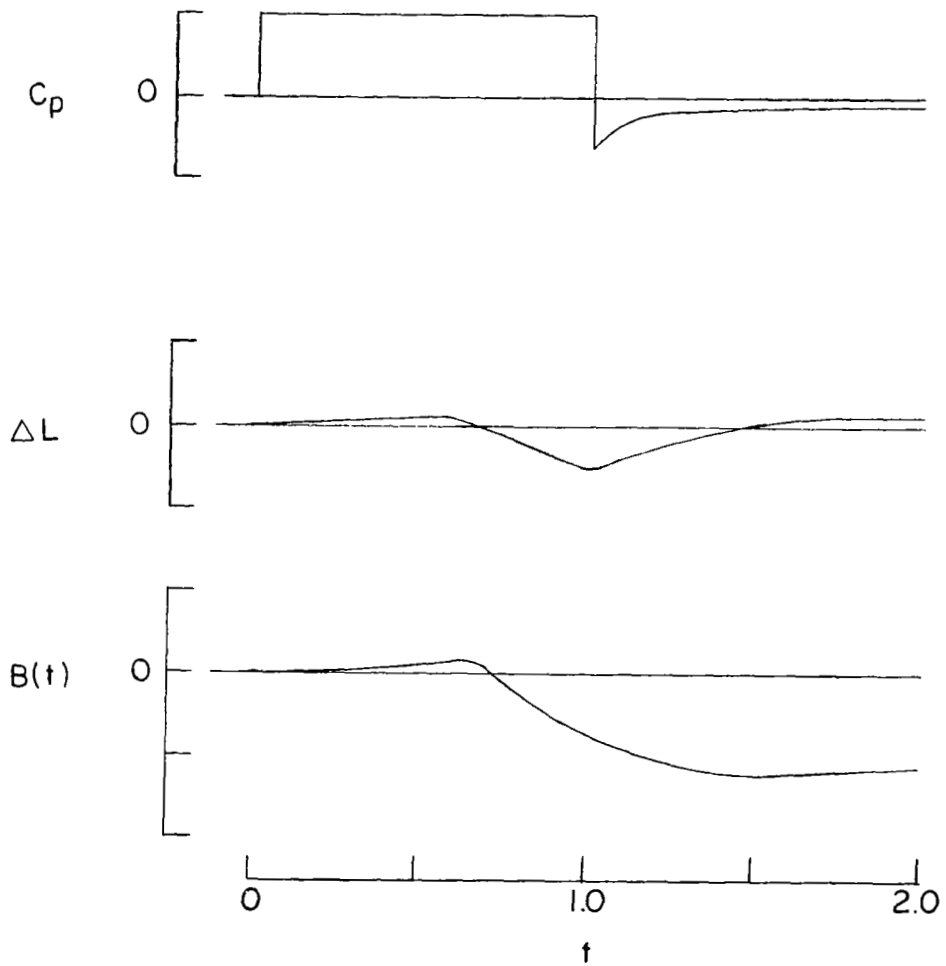
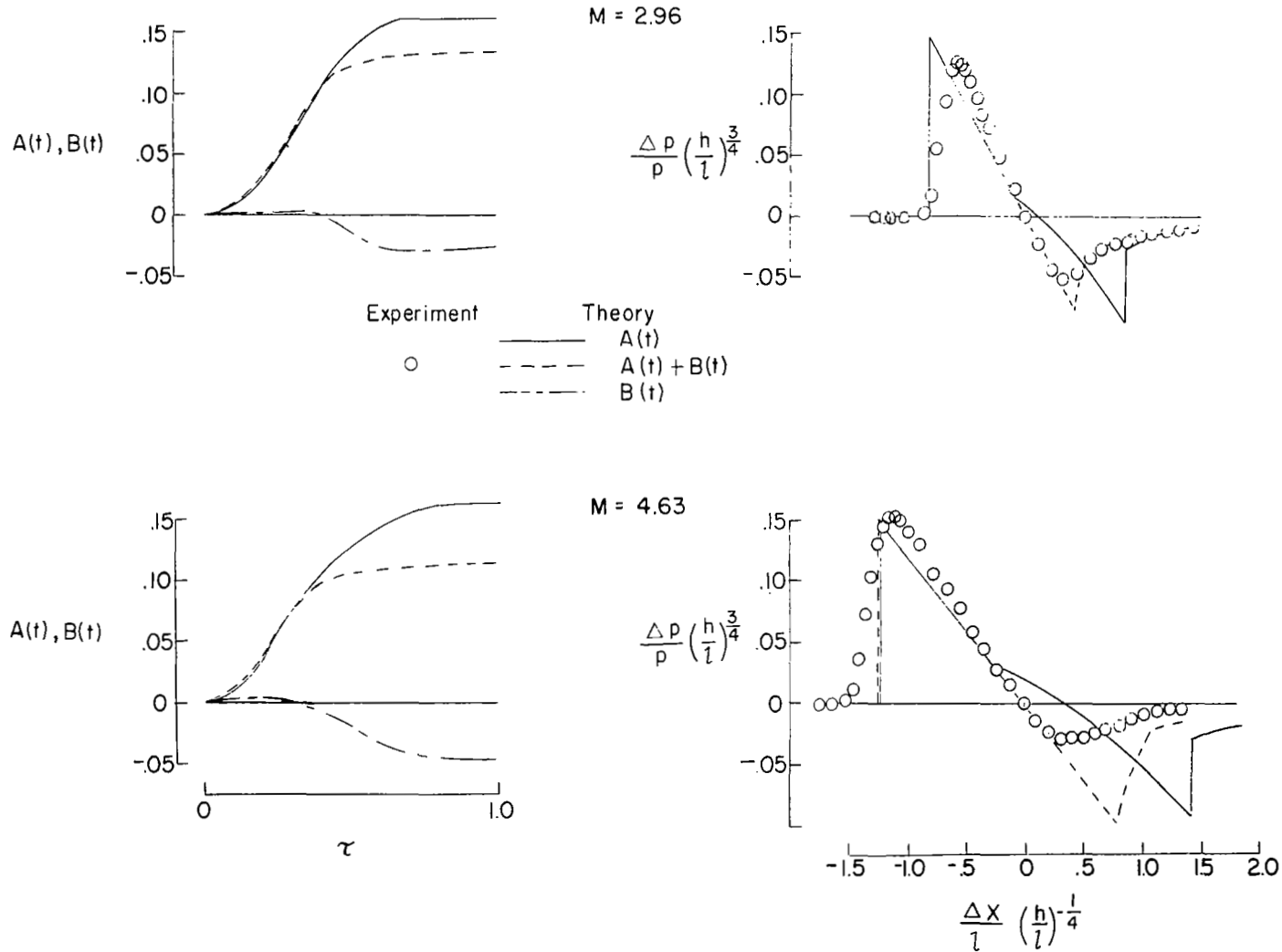Figure 13.- Schematic of equivalent lift on body of revolution.

M = 2.96

$A(t), B(t)$

$\dfrac{\triangle p}{p}\left(\dfrac{h}{l}\right)^{\frac{3}{4}}$

Experiment   Theory

○   —————— $A(t)$

    — — — — $A(t) + B(t)$

    —·——·— $B(t)$

M = 4.63

$A(t), B(t)$

$\dfrac{\triangle p}{p}\left(\dfrac{h}{l}\right)^{\frac{3}{4}}$

τ

$\dfrac{\triangle x}{l}\left(\dfrac{h}{l}\right)^{-\frac{1}{4}}$

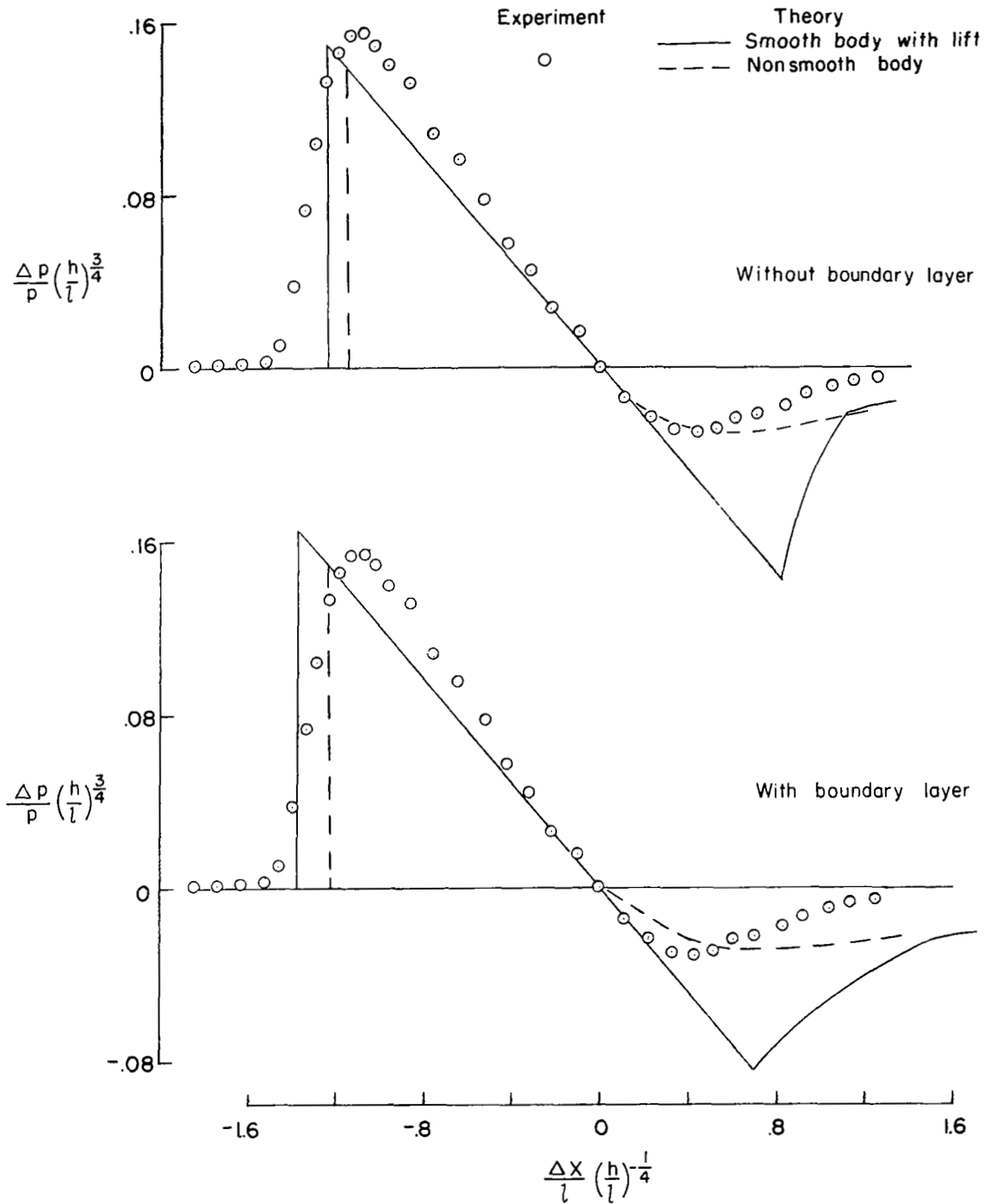Figure 14.- Effect of equivalent lift on area distributions and pressure signatures.   Model 7; $h/l = 5$.

Figure 15.- Comparison of smooth-body program with lift and nonsmooth-body program, with and without boundary layer. Model 7; M = 4.63; h/l = 5.

"The aeronautical and space activities of the United States shall be conducted so as to contribute . . . to the expansion of human knowledge of phenomena in the atmosphere and space. The Administration shall provide for the widest practicable and appropriate dissemination of information concerning its activities and the results thereof."

— NATIONAL AERONAUTICS AND SPACE ACT OF 1958

NASA SCIENTIFIC AND TECHNICAL PUBLICATIONS

TECHNICAL REPORTS: Scientific and technical information considered important, complete, and a lasting contribution to existing knowledge.

TECHNICAL NOTES: Information less broad in scope but nevertheless of importance as a contribution to existing knowledge.

TECHNICAL MEMORANDUMS: Information receiving limited distribution because of preliminary data, security classification, or other reasons.

CONTRACTOR REPORTS: Scientific and technical information generated under a NASA contract or grant and considered an important contribution to existing knowledge.

TECHNICAL TRANSLATIONS: Information published in a foreign language considered to merit NASA distribution in English.

SPECIAL PUBLICATIONS: Information derived from or of value to NASA activities. Publications include conference proceedings, monographs, data compilations, handbooks, sourcebooks, and special bibliographies.

TECHNOLOGY UTILIZATION PUBLICATIONS: Information on technology used by NASA that may be of particular interest in commercial and other non-aerospace applications. Publications include Tech Briefs, Technology Utilization Reports and Technology Surveys.

Details on the availability of these publications may be obtained from:

SCIENTIFIC AND TECHNICAL INFORMATION OFFICE

NATIONAL AERONAUTICS AND SPACE ADMINISTRATION
Washington, D.C. 20546